Supporting Information

Low-Temperature Direct Growth of Amorphous Boron Nitride films for High-Performance Nanoelectronic Device Applications

Seyed Mehdi Sattari-Esfahlan[1,2,3], Hyoung Gyun Kim[2], Sang Hwa Hyun[1,4], Jun-Hui Choi[1,4], Hyun Sik Hwang[1,4], Eui-Tae Kim[5], Hyeong Gi Park[6], and Jae-Hyun Lee[1,4]***

[1]Department of Material Science and Engineering, Ajou University, Suwon 16499, Republic of Korea

[2]Department of Materials Science and Engineering, Seoul National University, Seoul 08826, Republic of Korea

[3]Institute for Microelectronics, TU Wien, Vienna 1040, Austria

[4]Department of Energy Systems Research, Ajou University, Suwon 16499, Korea

[5]Department of Materials Science and Engineering, Chungnam National University, Daejeon 34134, Korea

[6]AI-Superconvergence KIURI Translational Research Center, Ajou University School of Medicine, Suwon 16499, Korea

Corresponding authors:

Hyeong Gi Park (hgpark007@ajou.ac.kr)

Jae-Hyun Lee (jaehyunlee@ajou.ac.kr)

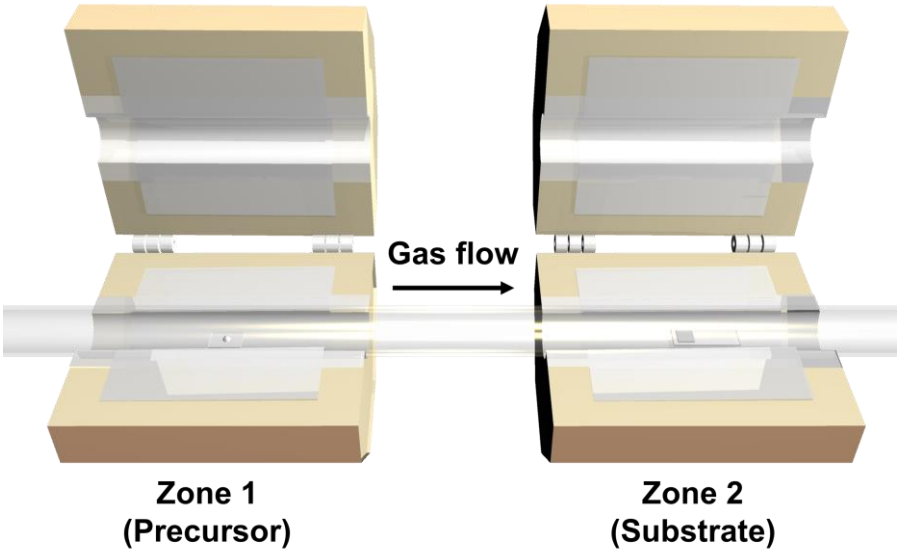

Figure S1 Single crystal graphene growth on the Ge substrate. Schematic illustration for the growth of graphene film using double-zone LPCVD. First, we prepared Ge substrate; to obtain high-quality graphene, the Ge (110) (0.5 mm-thick, n-type Sb doped) substrate was loaded in Zone 2 after the cleaning process (cleaned by ethanol, acetone, and methanol by ultrasonic for 10 min, respectively and then organic impurities are removed through O_2 plasma treatment). The temperature and pressure of Zone 2 were maintained at 920 °C and 100 Torr, respectively, and an H_2/CH_4 (99.999%, 200/4 sccm) mixture gas was introduced. After the growth process was completed, Zone 2 was rapidly cooled to room temperature in the H_2 atmosphere.

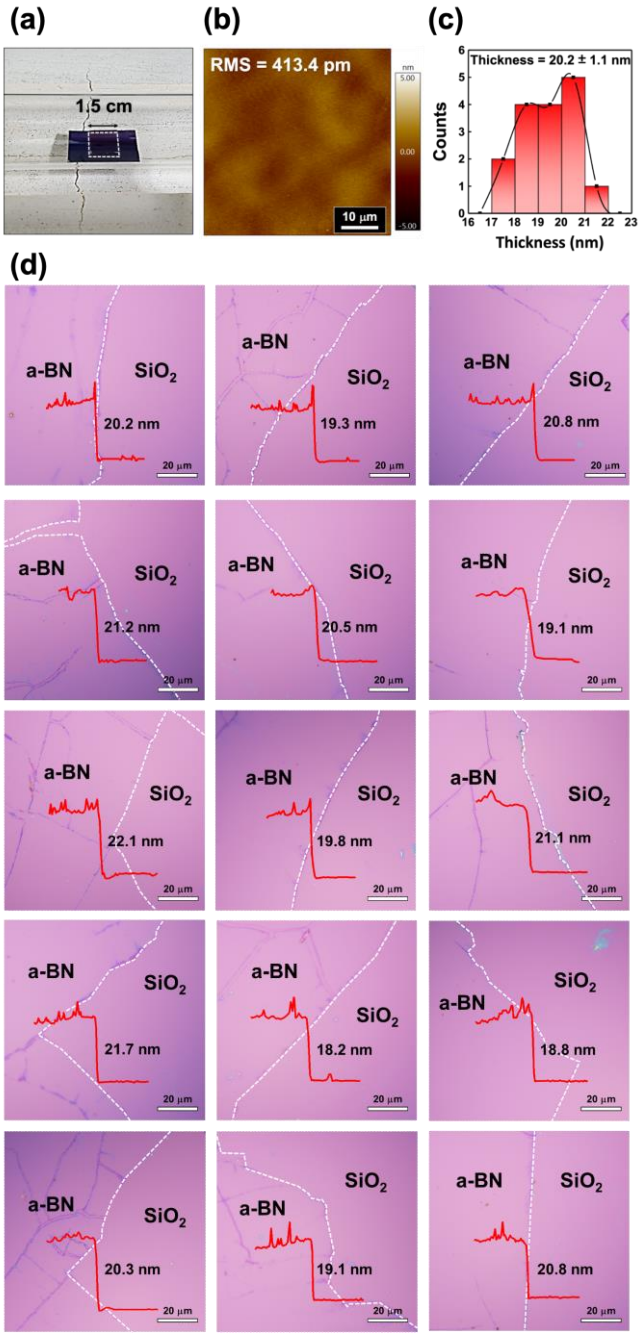

Figure S2 Uniform growth of a-BN film on the substrate. (a) Photo image of a-BN grown SiO_2/Si substrate (1.5 x 1.5 cm^2). (b) AFM image of the as-grown a-BN surface obtained from the region indicated with a white arrow in (a). We observed that the average root mean square (RMS) roughness of the a-BN measured by AFM is about 413 pm. (c,d) Height statistical analysis of a-BN samples. We prepared 15 a-BN samples under the optimized growth condition as described in main text and measured the height of them. Average thickness of a-BN film is about 20.0 nm, and its standard deviation is 1.1 nm.

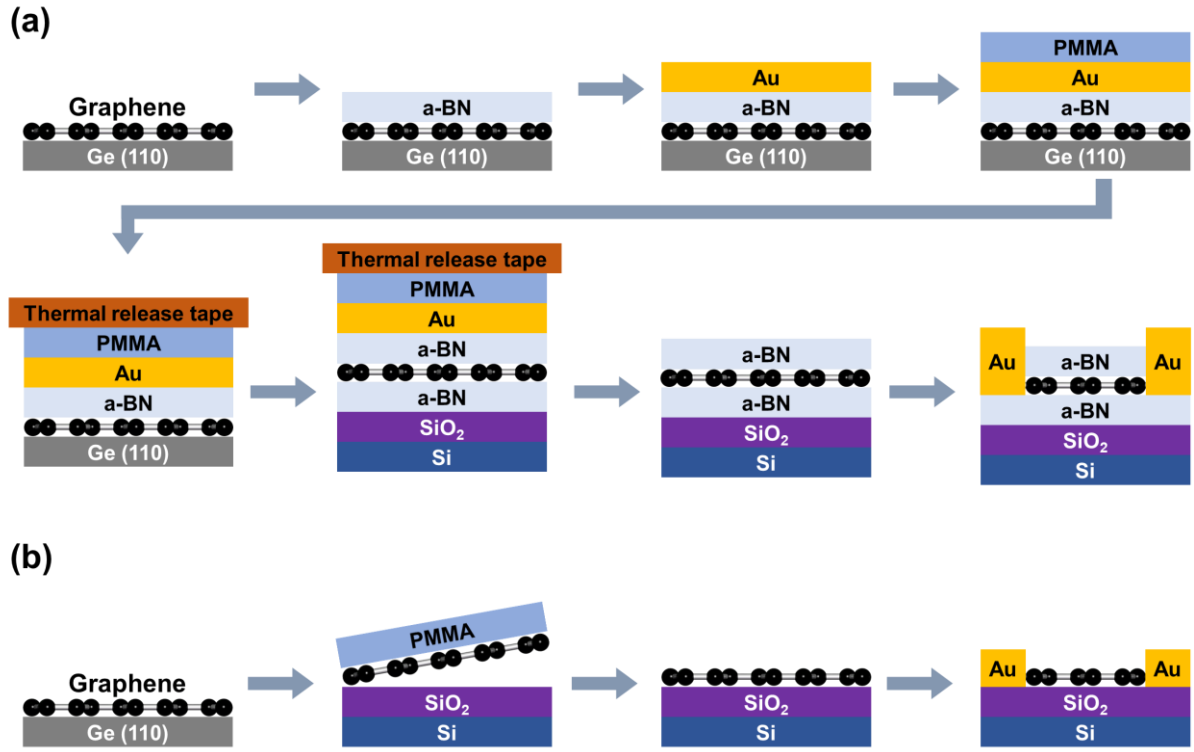

Figure S3 Fabrication process for Gr/SiO_2 and a-BN/Gr/a-BN FET devices. (a) Schematic illustration for encapsulation and device fabrication processes of a-BN/Gr/a-BN. (b) Schematic illustration for device fabrication processes of Gr/SiO_2. For comparison, we fabricated a graphene FET device based on Gr/SiO_2 sample. After graphene is grown on Ge substrate, we spin-coated PMMA on the graphene and baked at 120°C. The bottom Ge substrate was etched away by the mixture of H_2O_2 and HF solutions. The PMMA/Gr films were then floated on the DI water for 10 min and transferred onto the SiO_2/Si substrate. The two-terminal structure was patterned by standard photolithography (width: 2.0 μm and length: 3.0 μm). A thermal evaporator was used to deposit 15 nm Cr and 85 nm Au metals as metal electrodes for the source and drain of the FET devices. The graphene FET (GFET) was annealed at 180 °C for 1.5 hours to enhance the adhesion between the electrodes and the graphene channel, and to eliminate the oxygen functional groups adsorbed on the graphene surface

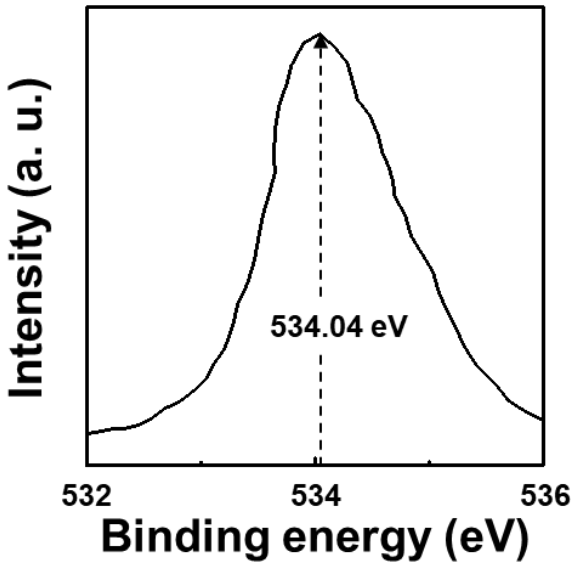

Figure S4 O1s peak acquired from the bare SiO_2/Si substrate.

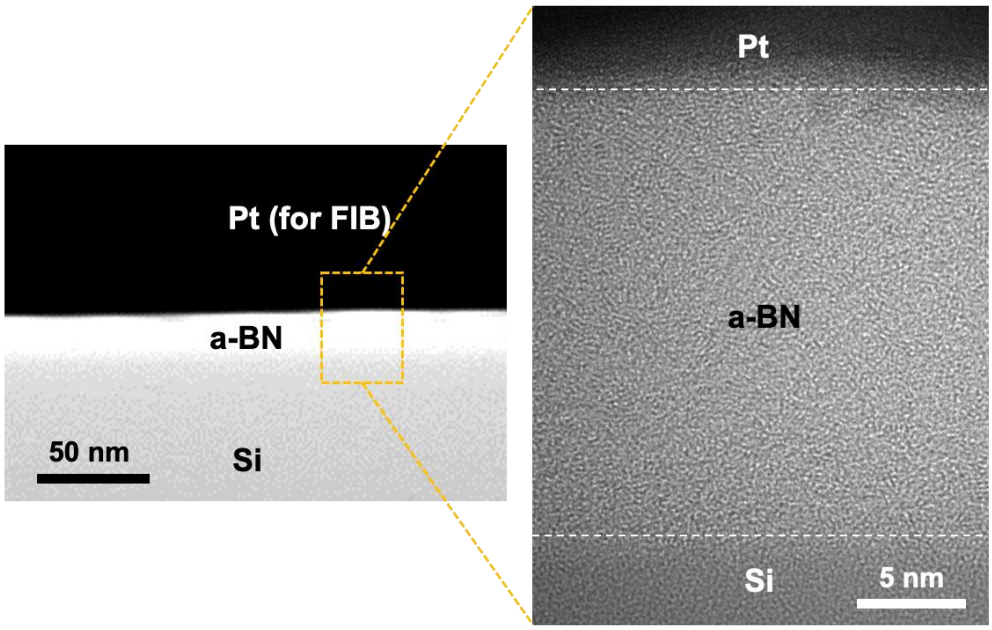

Figure S5 Cross-sectional HR-TEM image of the a-BN film on a Si substrate. (a) low-magnification and (b) high-magnification cross-sectional HR-TEM image of a-BN film on Si substrate for capacitance measurements. It should be noted that three a-BN samples were obtained from the same batch.

Table S1. Comparison of the carrier mobility of reported GFET with h-BN.

Device structure	Type of h-BN	h-BN growth temperature	Type of Graphene	Mobility (cm^2/Vs)@RT	Ref
Gr/h-BN	Mechanical exfoliation	N/A	Mechanical exfoliation	< 140,000	[1]
Gr/h-BN	Mechanical exfoliation	N/A	Mechanical exfoliation	28,630	[2]
Gr/h-BN	Mechanical exfoliation	N/A	Mechanical exfoliation	6,000	[3]
h-BN/Gr/h-BN	Mechanical exfoliation	N/A	Mechanical exfoliation	< 120,000	[4]
h-BN/Gr/h-BN	Mechanical exfoliation	N/A	Mechanical exfoliation	< 100,000	[5]
h-BN/Gr/h-BN	Mechanical exfoliation	N/A	Mechanical exfoliation	36,000	[6]
h-BN/Gr/h-BN	Mechanical exfoliation	N/A	Mechanical exfoliation	4,000	[7]
h-BN/Gr/h-BN	Mechanical exfoliation	N/A	CVD	70,000	[8]
h-BN/Gr	CVD	Commercial Product	CVD	5,000	[9]
h-BN/Gr	CVD	Commercial Product	CVD	4,140	[10]
h-BN/Gr	CVD	Commercial Product·	CVD	3,150	[11]
a-BN/Gr/a-BN	LPCVD	250˚C	CVD	< 17,000	This work

Table S2. Comparison of the different growth methods for a-BN films

Method	Growth Temp. (Pressure)	Properties of a-BN	Ref
PVD (PLD[1])	200 ºC (50 mTorr)	Dielectric constant 5.9±0.7 at 1 kHz Breakdown voltage 9.8±1.0 MV/cm	[12]
PVD (PLD)	200 ºC (5 - 100 mTorr) + 400 ºC post-annealing process	Mobility enhancement of the graphene by capping of the a-BN film (single-side)	[13]
PVD (MS[2])	500 ºC (0.5 Pa)	vacuum-ultraviolet photodetection photo-responsivity 4.8 μA/W at 10 V	[14]
ICP-CVD[3]	400 ºC (> 0.1 mTorr)	Dielectric constant 1.16 at 1 MHz Breakdown voltage 7.3 MV/cm	[15]
ICP-CVD	400 ºC (1.4 Torr)	Dielectric constant 2.11 at 100 kHz	[16]
PECVD[4]	350 ºC (N/A)	Bandgap 5 eV Breakdown voltage 2.2 MV/cm	[17]
LPCVD[5]	500 ºC (N/A)	Mobility enhancement of the 2D materials by capping of the a-BN film (single-side)	[18]
LPCVD	250 ºC (110 Torr)	Dielectric constant 1.25 at 1 MHz Mobility enhancement of the graphene by encapsulating of the a-BN film	This work

[1)]PLD: Pulsed Laser Deposition; [2)]MS: Magnetron sputtering; [3)]ICP-CVD: Inductively Coupled Plasma Chemical Vapor Deposition; [4)]PECVD: Plasma Enhanced Chemical Vapor Deposition; [5)]LPCVD: Low Pressure Chemical Vapor Deposition

References

[1] Dean, C. R.; Young, A. F.; Meric, I.; Lee, C.; Wang, L.; Sorgenfrei, S.; Watanabe, K.; Taniguchi, T.; Kim, P.; Shepard, K. L.; Hone, J. Boron nitride substrates for high-quality graphene electronics, *Nat. Nanotechnol.* **2010**, 5, 722-726.

[2] Xu, H.; Wu, J.; Chen, Y.; Zhang, H.; Zhang, J. Substrate Engineering by Hexagonal Boron Nitride/SiO_2 for Hysteresis-Free Graphene FETs and Large-Scale Graphene p-n Junctions, *Chem. Asian J.* **2013**, 8, 2446-2452

[3] Kayyahlha, M.; Chen, Y. P. Observation of reduced 1/f noise in graphene field effect transistors on boron nitride substates, *Appl. Phys. Lett.* **2015**, 107, 113101.

[4] Ponomarenko, L. A.; Geim, A. K.; Zhukov, A. A.; Jalil, R.; Novoselov.; Grigorieva, I. V.; Hill, E. H.; Cheianov, V. V.; Fal'ko, V. I.; Watanabe, K.; Taniguchi, T.; Gorbachev, R. V. Tunable Metal-Insulator Transition in Double-Layer Graphene Heterostructures, *Nat. Phys.* **2011**, 7, 958-961.

[5] Mayorov, A. S.; Gorbachev, R. V.; Morozov, S. V.; Britnell, L.; Jalil, R.; Ponomarenko, L. A.; Blake, P.; Novoselov, K. S.; Watanabe, K.; Taniguchi, T.; Geim, A. K. Micrometer-Scale Ballistic Transport in Encapsulated Graphene at Room Temperature, *Nano Lett.* **2011**, 11, 2396-2399.

[6] Stolyarov, M. A.; Liu, G.; Rumyantsev, S. L.; Shur, M.; Balandin, A. A. Suppression of 1/f noise in near-ballistic h-BN-graphene-h-BN heterostructure field-effect transistors, *Appl. Phys. Lett.* **2015**, 107, 023106.

[7] Neumann, C.; Reichardt, S.; Drögeler, M.; Terrés, B.; Watanabe, K.; Taniguchi, T.; Beschoten, B.; Rotkin, S. V.; Stampfer, C. Low B field Magneto-Phonon Resonances in Single-Layer and Bilayer Graphene, *Nano Lett.* **2015**, 15, 3, 1547-1552.

[8] De Fazio, D.; Purdie, D. G.; Ott, A. K.; Braeuninger-Weimer, P.; Khodkov, T.; Goossens, S.; Taniguchi, T.; Watanabe, K.; Livreri, P.; Koppens, F. H. L.; Hofmann, S.; Goykhman, I.; Ferrari, A. C.; Lombardo, A. High-Mobility, Wet-Transferred Graphene Grown by Chemical Vapor Deposition, *ACS Nano.* **2019**, 13, 8, 8926-8935.

[9] Giambra, M. A.; Mišeikis, V.; Pezzini, S.; Marconi, S.; Montanaro, A.; Fabbri, F.; Sorianello, V.; Ferrari, A. C.; Coletti, C.; Romagnoli, M. Wafer-Scale Integration of Graphene-Based Photonic Devices, *ACS Nano* **2021**, 15, 2, 3171-3187.

[10] Gao, X.; Yu, C.; He, Z.; Guo, J.; Liu, Q.; Zhou, C.; Cai, S.; Feng, Z. Contaminant-Free Wafer-Scale Assembled h-BN/Graphene van der Waals Heterostructures for Graphene Field-Effect Transistors, *ACS. Appl. Nano Mater.* **2021**, 4, 5677-5684.

[11] Shautsova, V.; Gilbertson, A. M.; Black, N. C. G.; Maier, S. A.; Cohen, L. F. Hexagonal

Boron Nitride assisted transfer and encapsulated of large area CVD graphene, *Sci. Rep.* **2016**, 6, 30210.

[12] Glavin, N. R.; Muratore, C.; Jespersen, M. L.; Hu, J.; Hagerty, P. T.; Hilton, A. M.; Blake, A. T.; Grabowski, C. A.; Durstock, M. F.; McConney, M. E.; Hilgefort, D. M.; Fisher, T. S.; Voevodin, A. A. Amorphous Boron Nitride: A Universal, Ultrathin Dielectric For 2D Nanoelectronics, *Adv. Funct. Mater.* **2016**, 26, 2640-2647.

[13] Uddin, M. A.; Glavin, N.; Singh, A.; Naguy, R.; Jespersen, M.; Voevodin, A.; Koley, G. Mobility Enhancement in Graphene Transistors on Low Temperature Pulsed Laser Deposited Boron Nitride, *Appl. Phys. Lett.* **2015**, 107, 203110.

[14] Li, Y.; Guo, J.; Huang, F. Amorphous Boron Nitride for Vacuum-Ultraviolet Photodetection, *Appl. Phys. Lett.* **2020**, 117, 023504.

[15] Hong, S.; Lee, C.-S.; Lee, M.-H.; Lee, Y.; Ma, K. Y.; Kim, G.; Yoon, S. I.; Ihm, K.; Kim, K.-J.; Shin, T. J.; Kim, S. W.; Jeon, E.-C.; Jeon, H.; Kim, J.-Y.; Lee, H.-I.; Lee, Z.; Antidormi, A.; Roche, S.; Chhowalla, M.; Shin, H.-J.; Shin, H. S. Ultralow-dielectric-constant amorphous boron nitride, *Nature* **2020**, 582, 511-514.

[16] Lin, C.-M.; Hsu, C.-H, Huang; W.-Y.; Astié, V.; Cheng, P.-H.; Lin, Y.-M.; Hu, W.-S. Chen, S.-H.; Lin, H.-Y.; Li, M.-Y.; Magyari-Kope, B.; Yang, C.-M.; Decams, J.-M.; Lee, T.-L.; Gui, D.; Woon, W.-Y.; Lin, P.; Wu, J.; Lee, J.-J.; Liao, S. S.; Cao, M. Ultralow-k Amorphous Boron Nitride Based on Hexagonal Ring Stacking Framework for 300 mm Silicon Technology Platform, *Adv. Mater. Technol.* **2022**, 7, 2200022.

[17] Zedlitz, R.; Heintze, M.; Schubert, M. B. Properties of Amorphous Boron Nitride Thin Films, *J. Non-Cryst. Solids,* **1996**, 198-200, 403-406.

[18] Lu, Z.; Zhu, M.; Liu, Y.; Zhang, G.; Tan, Z.; Li, X.; Xu, S.; Wang, L.; Dou, R.; Wang., B.; Yao, Y.; Zhang, Z.; Dong, J.; Cheng, Z.; Chen, S. Low-Temperature Synthesis of Boron Nitride as a Large-Scale Passivation and Protection Layer for Two-Dimensional Materials and High-Performance Devices, *ACS Appl. Mater. Interfaces* **2022**, 14, 22, 25984–25992.